Journal of the Institute of Energy, March 1990, pp 39–47

Predictions of nitric oxide emissions from an industrial glass-melting furnace

M G CARVALHO*, V SEMIAO*, F C LOCKWOOD** and C PAPADOPOULOS**

A mathematical model predicting the performance of the combustion chamber of industrial glass furnaces is described. The three-dimensional flow, gas composition, temperature field and heat fluxes are calculated by means of time-averaged forms of the governing conservation equations, in addition to the two-equation k-ϵ model for turbulent transport. The flame is modelled as a turbulent-diffusion flame, and the chemical reactions associated with the heat release are assumed to be fast. The fluctuations of the scalar properties are accounted for by the use of a clipped-Gaussian probability density function. The thermal radiation, which plays the dominant role in the heat-transfer process inside these furnaces, is accounted for by the use of the 'discrete transfer method'. The Zeldovich mechanism is incorporated in the model in order to predict the formation of the thermal NO from atmospheric nitrogen. This is the first time that predictions for NO emissions have been obtained for a cross-fired regenerative furnace.

1 List of symbols

g_i	gravitational acceleration in the i direction
$\bar{h}$	time-mean stagnation enthalpy
k	reaction rate
k	turbulent kinetic energy
M_j	molecular weight of the species j
m_j	time-averaged mass concentration of species j
p	pressure
$\bar{Q}_{rad}$	thermal radiation volumetric source
R_o	universal gas constant
S	source term
T	temperature
u_i	velocity component in the i direction
x_i	co-ordinate direction
Γ_φ	molecular exchange coefficient for a variable
δ_{ij}	Kronecker's delta
ε	dissipation rate of turbulent energy
μ	molecular viscosity
ρ	time-mean density
ρ_{ref}	density reference value
′	fluctuation component
¯	time-averaged value

2 Introduction

2.1 Preamble

Traditionally, the design of combustors has been based on the use of empirical models that attempt to correlate overall performance in terms of a number of simple global parameters — such as combustor volume, air-inlet temperature and pressure, mass flow rate and fuel:air ratio. However, a more fundamental approach is required both by the need for energy savings and by the necessity to reduce the emission of pollutants from such systems.

On oxidation, the combustion process would ideally convert all the sulphur to SO_2, the nitrogen to NO, the hydrogen to water and the carbon to CO_2. Combustion is not ideal, however, and the analysis of the combustion products reveals the presence of products such as SO_2, SO_3, NO, NO_2, CO, CO_2, H_2O, H_2, unburned hydrocarbons, polycyclic aromatic hydrocarbons and soot. Most these are pollutants.

Current emphasis on the reduction of combustion-generated pollutant emissions resulted in a renewed interest in the development of prediction methods for calculating the flow, gas composition, temperature and heat fluxes in practical combustion systems. Modelling of combustion in practical systems requires reliable models for the turbulence and for the combustion processes. Additionally, if the prediction of the pollutant emission is desirable, the interaction between turbulence and chemical kinetics must also be considered.

The major portion of NO_x in practical systems has been found to be NO[1]. This is the reason for the numerous analytical and experimental studies that have been focused on NO formation. Nitrogen oxide emissions emanate from two principal sources: i) the automobile, which is considered the major producer and for which emissions standards are enforced; and ii) stationary combustion chambers, such as those of electricity-generating plants and glass furnaces.

Because the research on NO kinetics and modelling has been so extensive, a review of some of the related papers is presented.

2.2 The kinetics of NO formation

The kinetics of NO formation from atmospheric nitrogen have been studied extensively. Early investigations[2] determined the mechanism of NO formation in combustion of fuel-oxygen-nitrogen mixtures. More recent studies on the kinetics of NO formation in laboratory flames support the Zeldovich mechanism (see References 3-8). However, Fenimore[9] has reported that in the vicinity of the combustion zone, NO formation rates exceeded those predicted by the Zeldovich mechanism. Rapidly formed NO, termed 'PROMPT' NO, was suggested to originate from reac-

*Instituto Superior Tecnico, Seccao de Termodinamica Aplicada, Av Rovisco Pais, 1096 Lisboa Cedex, Portugal
**Imperial College of Science Technology and Medicine, Mechanical

tions between nitrogen and CH radicals followed by oxidation. Later investigations[4] have justified the above-mentioned excess of NO formation by the presence of radicals in levels above their equilibrium values.

The work of Westenberg[3] presents a study of the NO kinetics in lean, premixed hydrocarbon-air flames, and deduced a model based on the assumption of constant temperature and equilibrium for the oxygen-atom concentration; the importance of low temperature in controlling the NO rate was emphasised in his work. Both thermal and fuel-bound nitric-oxide mechanisms have been investigated by Bowman[4]. In his work he found, after detailed comparisons of kinetics calculations and experiments, that the Zeldovich mechanism was the determining one in the thermal NO formation. The work of Flower *et al*[5] has demonstrated the importance of the hydrogen-atom concentration on the NO reduction in the temperature range 2400-4500 K, especially for fuel-rich mixtures.

A detailed kinetic model, involving fifteen chain reactions and species containing hydrogen, oxygen and nitrogen, was obtained for flames of that class. The presence of radicals in super-equilibrium — that is in levels above their equilibrium values — is a matter of present-day research. The importance of the presence of super-equilibrium radicals (namely the OH radical) on the thermal NO formation has been demonstrated by Drake *et al*[6]. Finally it was concluded that NO is formed in the near-stoichiometric flame zone in turbulent-diffusion flames, and that the degree of super-equilibrium of radicals, similar to premixed flames, decreases when the peak flame temperature increases.

2.3 NO modelling in practical systems

A two-dimensional mechanistic model was presented by Katsuki *et al*[10] to study the NO formation rate and its dependence on temperature and species concentration, in a gas-turbine combustor using the Zeldovich mechanism. The calculations of the combustion aerodynamics were based on the simplified hypothesis of: a boundary layer approximation in the main flow region, no reversed flow outside the recirculation zone, a single step and equilibrated reaction for the oxidation of the fuel in the absence of radiative heat-transfer effects and the turbulence being modelled by an empirical correlation.

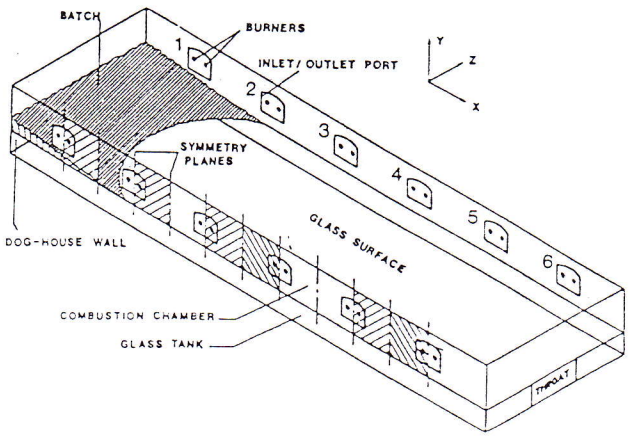

Peters[11], although exploiting the fact that NO is formed in a narrow region around the maximum temperature in turbulent-diffusion flames, determined the NO formation rate by an asymptotic expansion in terms of a small parameter δ, using the Zeldovich mechanism. A two-dimensional axisymmetrical model was used, and the predictions agree favourably with experimental results for a hydrogen-air jet diffusion flame, despite the use of an empirical correlation for the turbulent-viscosity calculations. A three-dimensional model was presented by Jones & Priddin[12], in which the Favre-averaged forms of the governing conservation equations and the k-ε two equations for turbulent transport are solved in order to predict a gas-turbine combustor. The combustion model was based on the fast kinetics assumption and the fluctuations in scalar properties being accounted for by the use of a Beta probability density function. Radiative heat transfer was not considered.

The Zeldovich NO mechanism was employed. Surprisingly, comparisons with experimental values have shown that the model over-estimated the NO concentration, although the possibility of super-equilibrium of radicals was not allowed for. The model presented by Drake *et al*[6] is similar to the model of Jones & Priddin[12]—the same turbulence model, a fast kinetics assumption for the combustion model with the turbulent fluctuations accounted for by an assumed pdf, the thermal NO calculated from the Zeldovich mechanism, but with a new kinetic model introduced for the production of NH_2.

A model similar to the previous ones was presented by Ahmad *et al*[13], but in this case the authors have also calculated the spatial distribution of the soot. They applied it to the calculations of a turbulent jet-diffusion flame. The conclusion of their work was the importance of simulating the influence of turbulence on the chemical kinetics. None of the above-mentioned authors considered the effects of the reverse reactions of the Zeldovich mechanism.

In spite of numerous works on the modelling of NO emissions, their application has been restricted to gas-turbine combustors and diesel engines. The present work presents a three-dimensional simulation of an industrial glass furnace under real operating conditions. Time-averaged forms of the governing conservation equations along with the k-ε turbulence model are used.

The combustion model is based on the fast kinetics hypothesis, with turbulent fluctuations of scalars being accounted for by use of a clipped Gaussian pdf. Radiative heat transfer is allowed for by the discrete transfer method. The time-averaged NO mass concentration is calculated by solution of its conservation transport equation. The Zeldovich mechanism is used to simulate the NO formation rate; for the first time, the reverse reactions are retained.

2.4 Description of the furnace

Fig. 1 shows the furnace, which is of the cross-fired regenerative kind. This furnace is essentially a large insulated container in which the batch enters via the 'dog-house wall' and the molten glass exits from the opposite end. The firing ports are located along the sides of the furnace. There are

The furnace is fired alternately from either side to ensure uniform heat flux to the glass and to facilitate the regeneration process.

The combustion products pass through the regenerators, which are used to preheat the combustion air before entering the furnace and to produce higher temperatures and augment the heat flux to the glass. The wall openings surrounding the burners serve alternately as air-entry locations and waste-gas exits as the firing direction is altered. Methane fuel is burned with excess air, at typical values in the range 8-12%. The roof of the furnace and the side walls are refractory lined.

3 Physical modelling

The governing transport equations for the mean motion of a turbulent three-dimensional flow were applied in their Cartesian form. The time-averaged equations for the conservation of momentum in compact tensor notation, are:

$$\frac{\partial}{\partial x_j}\left(\overline{\rho u_j u_i} + \bar{p}\delta_{ij} - \mu\left[\frac{\partial \bar{u}_i}{\partial x_j} + \frac{\partial \bar{u}_j}{\partial x_i} - \frac{2}{3}\frac{\partial \bar{u}_k}{\partial x_k}\delta_{ij}\right]\right) +$$

$$-\left(\bar{\rho} - \rho_{ref}\right)g_i + \frac{\partial}{\partial x_j}\left(\overline{\rho u_j' u_i'}\right) = 0 \qquad (1)$$

where u_i is the velocity component in the direction of coordinate x_i, ρ is density and ρ_{ref} a reference value, g_i is the magnitude of the gravitational acceleration in the i direction, p is pressure, μ is the laminar viscosity, and the operator δ_{ij} is unity for i = j, and zero when i ≠ j.

The equation for the conservation of energy may be expressed as:

$$\frac{\partial}{\partial x_j}\left(\overline{\rho u_j \tilde{h}}\right) - \frac{\partial}{\partial x_j}\left(\Gamma_h \frac{\partial \bar{h}}{\partial x_j}\right) + \frac{\partial}{\partial x_j}\left(\overline{\rho u_j' h'}\right) - \bar{Q}_{rad} = 0 \qquad (2)$$

where $\bar{h}$ represents the stagnation enthalpy, Γ_h is equal to the fluid's thermal conductivity divided by its constant-pressure specific heat, and $\bar{Q}_{rad}$ is the net volumetric heat gain due to thermal radiation.

In addition to equations (1)–(2) the continuity equation is cast as:

$$\frac{\partial}{\partial x_i}\left(\overline{\rho u_i}\right) = 0 \qquad (3)$$

The two-equation model[14], in which equations for the kinetic energy of turbulence, k, and its dissipation rate, ε, are solved, appears to be satisfactory for the present application[15]. The combustion model is based on the assumption that the reaction rates associated with the fuel oxidation have time scales that are very short relative to those describing the transport processes. Under these circumstances chemical equilibrium prevails. Assuming that all species and heat diffuse at the same rate, the instantaneous gas composition can be determined as a function of a conserved scalar variable[16]. Any conserved scalar may be chosen, so here the mixture fraction f is used, defined as the

In turbulent flow the mixture fraction fluctuates, and knowledge of its mean value is insufficient to allow the determination of the mean values of quantities such as density and temperature, because of the non-linearity of their relationships. A statistical approach is used to describe the temporal nature of the mixture fraction fluctuations. In the present work we have assumed the 'clipped' normal probability density function for the mixture fraction[17], which is completely defined by the knowledge of its mean value and variance, g. The variables f and g also obey transport equations.

The discrete transfer radiation prediction procedure has been utilised in this study. This procedure, which is fully described by Lockwood and Shah[18], is numerically exact, fast, and applicable to arbitrary geometries. The gas absorption coefficient is calculated from the 'two grey plus a clear gas' fit[19].

NO emission is greatly dependent on the flame structure. For premixed flames the temperature, and thus the mixture ratio, are the prime parameters in determining the NO quantities formed. The NO formation should peak at the stoichiometric value and decline on both the fuel-rich and fuel-lean sides as temperature does. In reality, because of non-equilibrium effects, the peak is found somewhat on the lean side of the stoichiometric value. The temperature of the diffusion flame is the stoichiometric value during part of the burning time, even though the excess oxygen will eventually dilute the products of the flame to reach the true equilibrium final temperature. Thus, in diffusion flames, more NO forms than would be expected from a calculation of an equilibrium temperature based on the overall mixture ratio.

As NO is present only in trace amounts, and it has negligible influence on the heat-releasing reactions and temperature, its calculation has been traditionally considered to be independent of those for the combustion aerodynamics. At high temperature—say in the range 1900 – 2500 K, which is the case for industrial furnaces—the thermal NO (undoubtedly the controlling mechanism of the NO formation) builds up by reactions that are slow relative to those of combustion; thus the modelling of NO concentration presumes a finite rate reaction. The usual assumption made for the combustion models of chemical equilibrium—complete combustion to form equilibrium products—is not valid here. For the present combustion model a turbulent diffusion flame is assumed, whereas the NO emission model demands a chemical approach.

As was previously stated, the kinetic route of NO formation is not the attack of oxygen molecules by nitrogen ones ($N_2 + O_2 \rightleftharpoons 2NO$). Mechanistically, oxygen atoms are formed from dissociation of O_2 or from the hydrogen atom attack on O_2. (See reactions (R1) and (R2) below.)

$$O + OH \Leftrightarrow O_2 + H \qquad (R1)$$

$$O_2 + M \Leftrightarrow O + O + M \qquad (R2)$$

The oxygen atoms that are formed will then attack the nitrogen molecules along the Zeldovich mechanism[2]:

$$O + N_2 \Leftrightarrow NO + N \qquad (R3)$$

Another reaction—which is less important, since reacting species are both radicals and therefore present only in very small quantities (see 4 and 5)—is the following one:

$$N+OH \Leftrightarrow NO+H \qquad (R5)$$

From the extended Zeldovich mechanism [(R3) to (R5)], and assuming steady state for the nitrogen atom concentration, the relation giving the NO production rate can be determined as a function of the rate constants K_3, K_4, K_5, K_{-3}, K_{-4}, K_{-5} where the minus sign stands for the reverse reactions. With $[N_2]$, $[O]$, $[NO]$, $[OH]$, $[H]$, $[O_2]$ standing for the respective concentrations, it runs:

$$\frac{d[NO]}{dt} = \frac{1}{1 + \frac{k_{-3}[NO]}{K_4[O_2] + K_5[OH]}} \qquad (4)$$

$$\left(2K_3[N_2][O] - \frac{2K_{-3}K_{-4}[NO]^2[O]}{K_4[O_2] + K_5[OH]} - \frac{2K_{-3}K_{-5}[NO]^2[H]}{K_4[O_2] + K_5[OH]}\right)$$

Furthermore, assuming **partial equilibrium** for (R1), justified by the high levels of temperature which prevents radicals overshoots[8], equation (4) becomes

$$\frac{d[NO]}{dt} = \frac{2K_3[N_2][O]\left(1 - \frac{[NO]^2}{K[O_2][N_2]}\right)}{1 + \frac{K_{-3}[NO]}{K_4[O_2] + K5[OH]}} \qquad (5)$$

where $k = K_3K_4/K_{-3}K_{-4}$. The values of $[N_2]$ and $[O_2]$ can be taken from the equilibrium values calculated by the combustion model. However, the $[O]$ and $[OH]$ concentrations still remain unknown. Partial equilibrium of (R2) is assumed, so:

$$[O] = \left[\frac{K_2}{K_{-2}}[O_2]\right]^{0.5} = [K_v[O_2]]^{0.5} \qquad (6)$$

The value of K_v was taken from the data reported by Baulch *et al*[20]:

$$K_v = 9.474\times10^{-4}\,T^{-1}\exp\left(-\frac{119800}{Ro\,T}\right)[\text{mole cm}^{-3}] \qquad (7)$$

Assuming partial equilibrium and that reaction R5 is significant only in rich flames, equation (5) becomes:

$$\frac{d[NO]}{dt} = \frac{2[O](K_3K_4[O_2][N_2] - K_{-3}K_{-4}[NO]^2)}{K_4[O_2] + K_{-3}[NO]} \qquad (8)$$

The last equation has been used in this work to model the NO formation rate. Note that in previous studies the reverse reactions of the Zeldovich mechanism were not taken into account. Ignoring these reactions results in overestimating the NO emissions for the present application.

The time-mean NO mass concentration is calculated from its conservation transport equation:

$$\frac{\partial}{\partial x_i}\overline{(\rho u_i m_{NO})} = \frac{\partial}{\partial x_i}\left(\Gamma_{NO}\overline{\frac{\partial m_{NO}}{\partial x_i}} + \overline{S_{NO}}\right) \qquad (9)$$

The time-average source term S_{NO} is found by convoluting S_{NO}. The value of S_{NO} is given by:

TABLE 1: The Zeldovich mechanism rate constants

Reaction	K [cm^3 mole^{-1} sec^{-1}]
R3	$K_3 = 1.36 \times 10^{14} \exp\left(-\frac{75400}{R_oT}\right)$
R4	$K_4 = 6.43 \times 10^9\, T \exp\left(-\frac{6250}{R_oT}\right)$
R−3	$K_{-3} = 3.1 \times 10^{13} \exp\left(-\frac{334}{R_oT}\right)$
R−4	$K_{-4} = 1.55 \times 10^9\, T \exp\left(-\frac{38640}{R_oT}\right)$

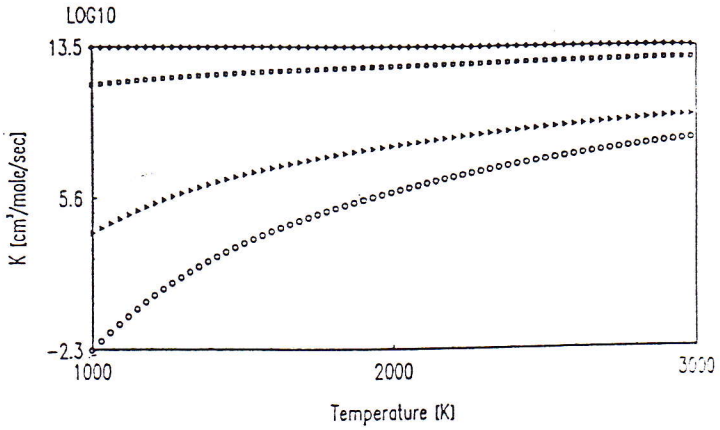

Fig.2 The rate reactions constants of the Zeldovich mechanism:
Reaction R3 ○
Reaction R-3 ◇
Reaction R4 □
Reaction R-4 ▷

The constants appearing in equation (8) were taken from Baulch *et al*[20], and are presented in Table 1. These constants have been plotted as a function of temperature in Fig.2. This figure shows that the reactions R3 and R-4 are the controlling ones, as they are the slowest. Fig.2 shows that above 1400 K the decomposition of NO through reaction R-4 is almost homogeneous.

4 The numerical solution procedure

4.1 Method of solution

The finite-difference method used to solve the equations entails subdividing the calculation domain into a number of finite volumes or 'cells'. Convection terms are modelled along the hybrid central/upwind method, and the velocities and pressures are calculated by a variant of the SIMPLE algorithm. The solution of the individual equation sets is obtained by a form of Gauss-Seidel line-by-line iteration.

4.2 Some computational details

Nearly all industrial furnaces are three-dimensional, and exhibit disparity of scales: most of the combustion takes place within a volume surrounding the burner that occupies only a small proportion of total furnace volume but requires a disproportionately large portion of the total computational grid. In order to avoid excessive memory requirements in the present study for a full-scale industrial glass furnace (Fig.1), the combustion chamber was

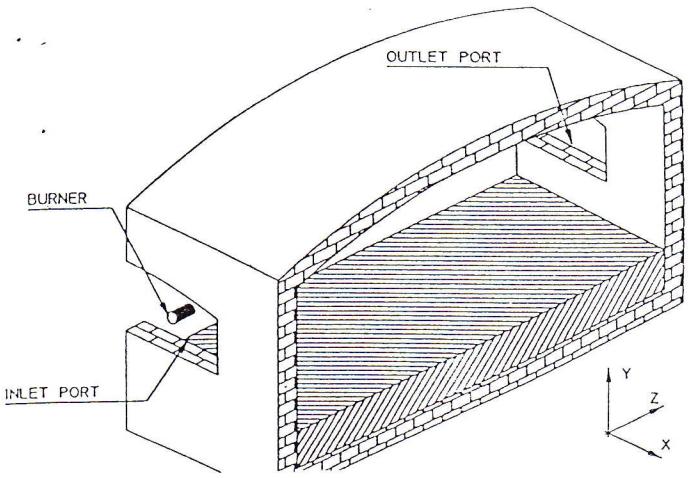

Fig.3 The numerical domain.

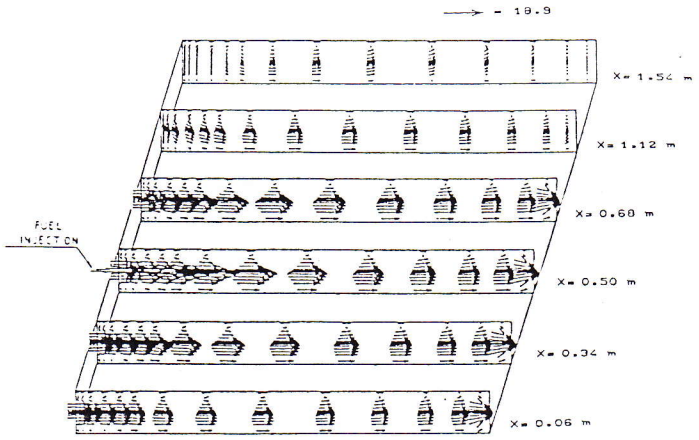

Fig.4(a) Velocity vectors projected on planes YZ.

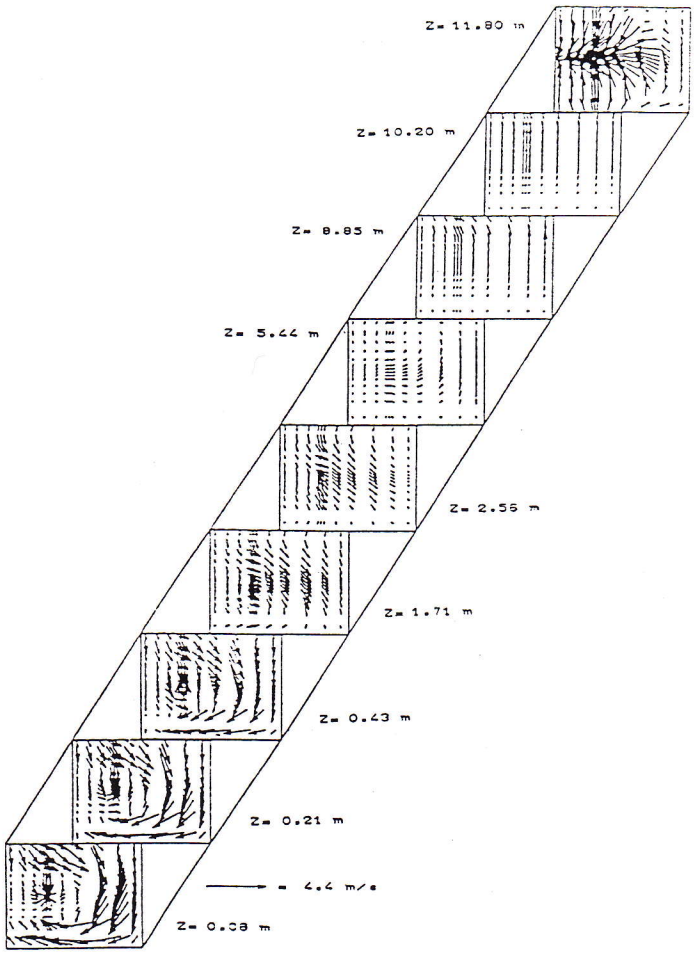

Fig.4(b) Velocity vectors projected on planes XZ.

between the midway plane of the inlet port and the midway plane halfway between this inlet port and the adjacent one, Fig.3. The results presented here correspond to the conditions of port No. 3 (Fig.1).

Because of the long period of the alternating firing-direction cycle, the transient nature of the firing process is neglected. The fuel is injected at the ambient temperature, and the air is pre-heated to 1450 K. The mass flow of fuel and air are 0.087 kg/s and 1.59 kg/s respectively. A prescribed glass-temperature distribution was used. The temperature distribution of the glass surface was taken from the calculations performed for a similar furnace[21]; in this work the phenomena occurring in the glass tank and the combustion chamber were modelled, thereby allowing calculation of the glass surface distribution.

The selection of the optimum finite-difference grid to predict the present flow is a complex task. The aim is to establish a grid with the smallest possible number of nodes, for which the finite-difference solutions are essentially those of the original differential equations. This is achieved in part by obtaining solutions with increasing number of grid nodes until a stage is reached where the solution exhibits negligible change with further increase in the number of nodes, or with small adjustments in their distribution. For each test a fully converged solution must be obtained, in order to make a valid comparison of the different grids employed.

5 Presentation and discussion of the results

Some general aspects of the predictions are illustrated in Figs.4-11.

5.1 Velocity

Fig.4(a) shows predicted projections of velocity vectors on vertical planes normal to the inlet port (ie on YZ planes), whereas Fig.4(b) shows the referred projections on vertical planes parallel to the inlet port (ie on XY planes). The first four planes on Fig.4(a) (0.06 m $<$ X $<$ 0.68 m) show that the flow is mainly a jet crossing the furnace from the inlet to the outlet port. A recirculation zone is found on the upper inverted. From the vectors presented in Fig.4 it is concluded that the flow is fully three-dimensional.

5.2 Temperature

Fig.5 shows the temperature distribution in vertical planes parallel to the inlet-port-containing wall. In the reaction zone the temperatures and the temperature gradients are higher than in the outer zones. Outside the flame region the temperature is nearly homogeneous. Temperatures are higher below the horizontal plane containing the burner than above it. This is due to the upper recirculation zone, which slightly directs the flame towards the glass over a

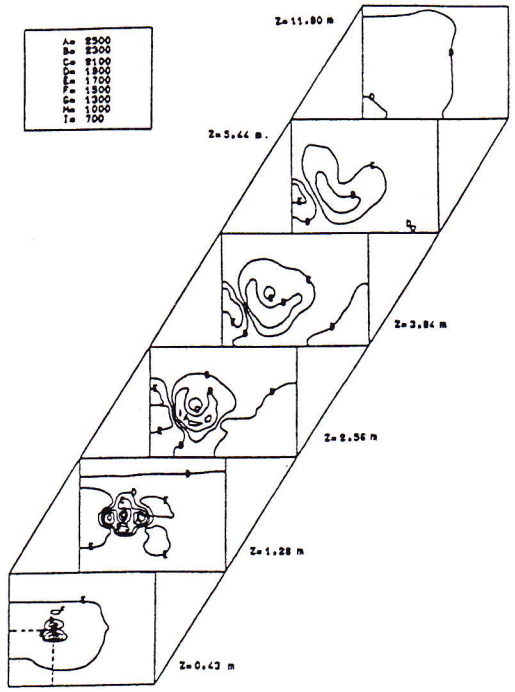

Fig.5 Temperature distribution (K) inside the furnace. The intersection point of the dashed lines identifies the position of the fuel injection.

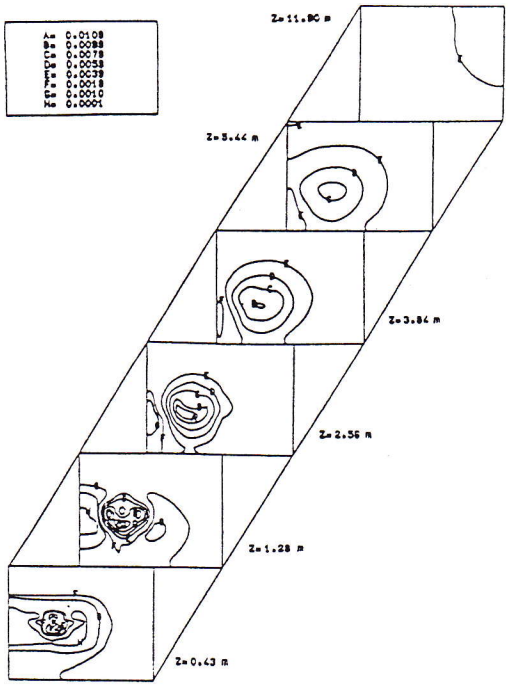

Fig.6 Mass concentration of nitric oxide inside the furnace. (kg_{NO}/kg_{mix})

5.3 Mass concentration of nitric oxide

Fig.6 contains the NO mass concentration in vertical planes parallel to the inlet-port-containing wall. The results show that the thermal NO is formed mainly at the edge of the flame, near the stoichiometric region, where the levels of temperature are high and the oxygen concentrations are still significant, as can be seen in Fig.7. The NO concentrations reach their maximum values near the flame front at a distance of about two metres downstream of the inlet port.

Further downstream the levels of NO are progressively reduced because of the convection and diffusion of NO away from the region where it is formed. Inside the upper recirculation zone, the NO mass concentration is uniform. At the outlet port, the predicted NO concentration is uniform with a value of 3.9×10^{-3} kg_{NO}/kg_{mix}.

5.4 Production rate of nitric oxide

In systems such as glass furnaces operating at high temperatures, there is a competition between nitrogen molecules and nitric oxide molecules to capture oxygen atoms. The net tendency of both opposing effects is a function of local temperature and local concentrations of oxygen, nitrogen and nitric oxide.

The present flame extends from the injection point to a position approximately 5.0 m downstream. The maximum width of the flame is about 10% of the total length, and the maximum flame temperature is 2500 K, attained at the location z = 3.9 m at the periphery of the flame.

Figs.8(a) to 8(c) contain the NO production-rate profiles for different locations within the combustion chamber. Figs.8(a) to 8(b) show that the NO is produced mainly in the first four metres after the inlet port, where the NO production rates exhibit their maximum values. However, downstream of that distance, and still within the flame zone, the profiles appear flatter—achieving almost zero values. The negative peaks that appear in different panels of Fig.8 represent the maximum rates of NO decomposition through the reaction R-4.

In sum, these results show that the production effect dominates in the outer edge of the flame where the temperatures are near to their maximum values, where oxygen still attains high concentration values and where nitrogen is

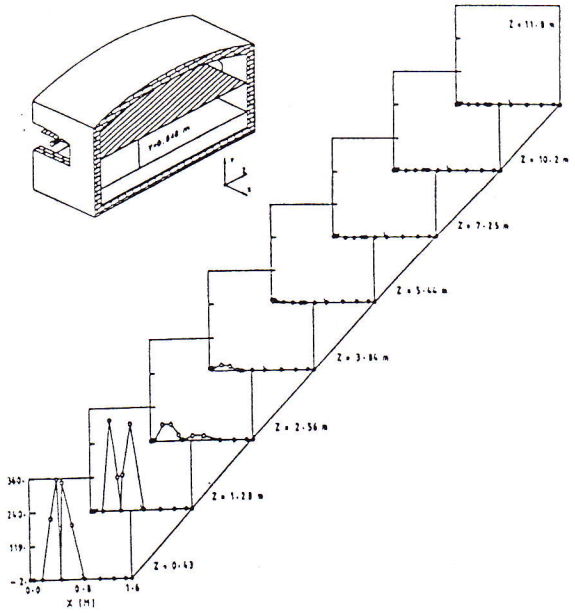

Fig.8(a) Nitric oxide production rate profiles for Y = 0.648 m plane. ($kg_{NO} \times 10^4\ m^{-3}s^{-1}$)

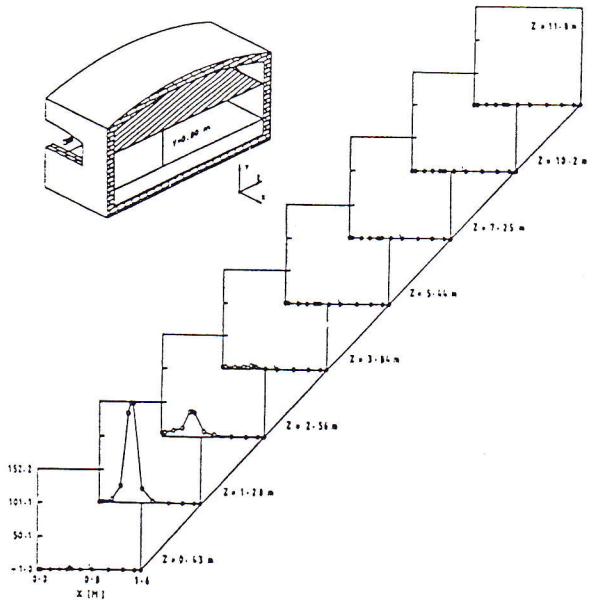

Fig.8(b) Nitric oxide production rate profiles for Y = 0.8 m plane. ($kg_{NO} \times 10^4\ m^{-3}\ s^{-1}$)

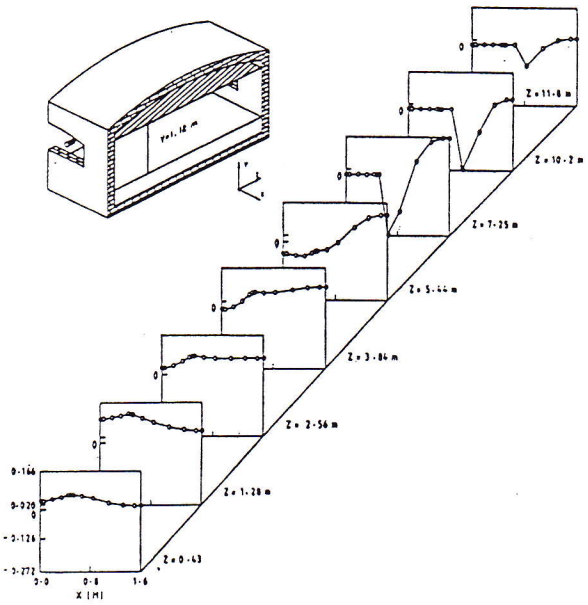

Fig.8(c) Nitric oxide production rate profiles for Y = 1.12 m plane. ($kg_{NO} \times 10^4\ m^{-3}\ s^{-1}$)

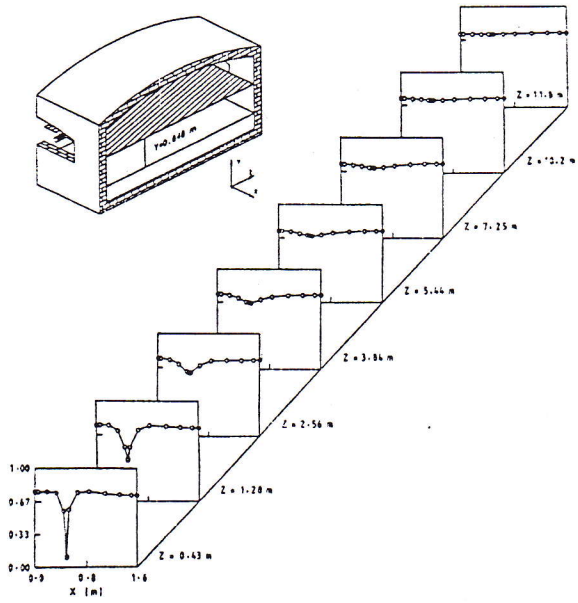

Fig.9 Nitrogen mass concentration profiles for Y = 0.648 m plane. (kg_{N2}/kg_{mix})

Conversely, in regions where temperature is still above 1400 K, the reaction $NO + O \rightarrow N + O_2$ takes place, where nitric oxide exists in considerable concentration and oxygen is still available, the decomposition effect plays an equal or dominant role compared with the production one. Downstream of the reaction zone the NO production rate achieves zero or negative values.

Note that the upper recirculation zone (where temperatures are high, oxygen appears in trace quantities and the NO attains significant values) the net rate production is about zero almost everywhere; in the downstream region ($Z \geq 7.25$ m) the decomposition effect slightly dominates

5.5 The effect of the reverse reaction

Panels (a) and (b) of Fig.10 contain profiles along X, for Y = 0.648 m and Z = 1.28 m for the NO mass concentrations and for the NO volumetric production rate. For the same conditions of temperature and species mass concentrations (these conditions are shown in panels c) to e) of the same Figure), the NO mass concentration and its production rate, calculated both with reverse reactions and without it, are presented. The results show that the reverse reactions must be included in the calculations of combustors operating at high temperature levels, as they play a relevant role in the whole NO formation process. Indeed, the omission of those reactions may lead to very large over-

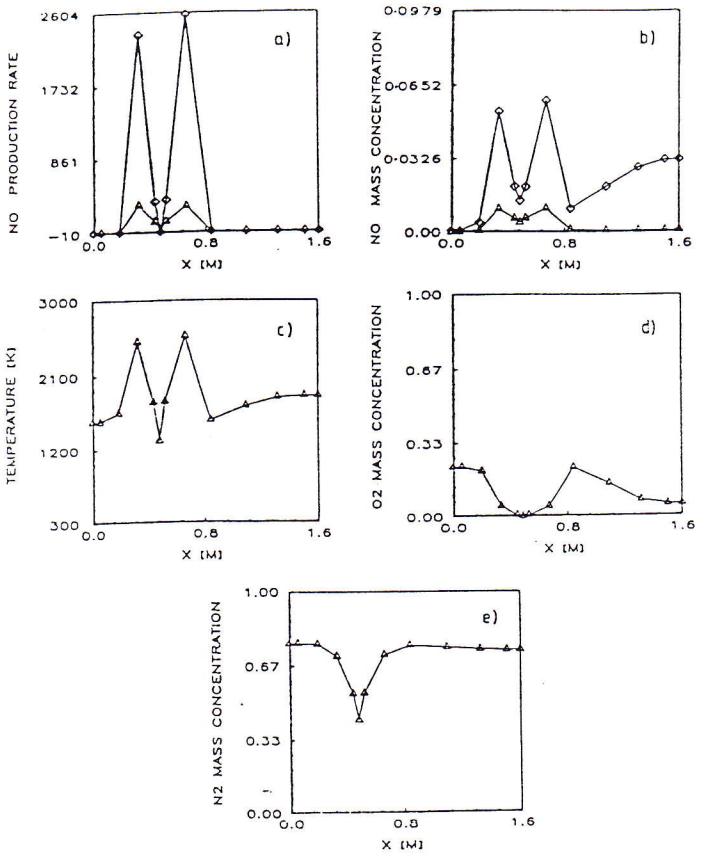

Fig.10 The effect of the reverse reactions in the front flame region. (Y = 0.648 m; Z = 1.28 m).
Results with the reverse reactions △
Results without the reverse reactions ◇

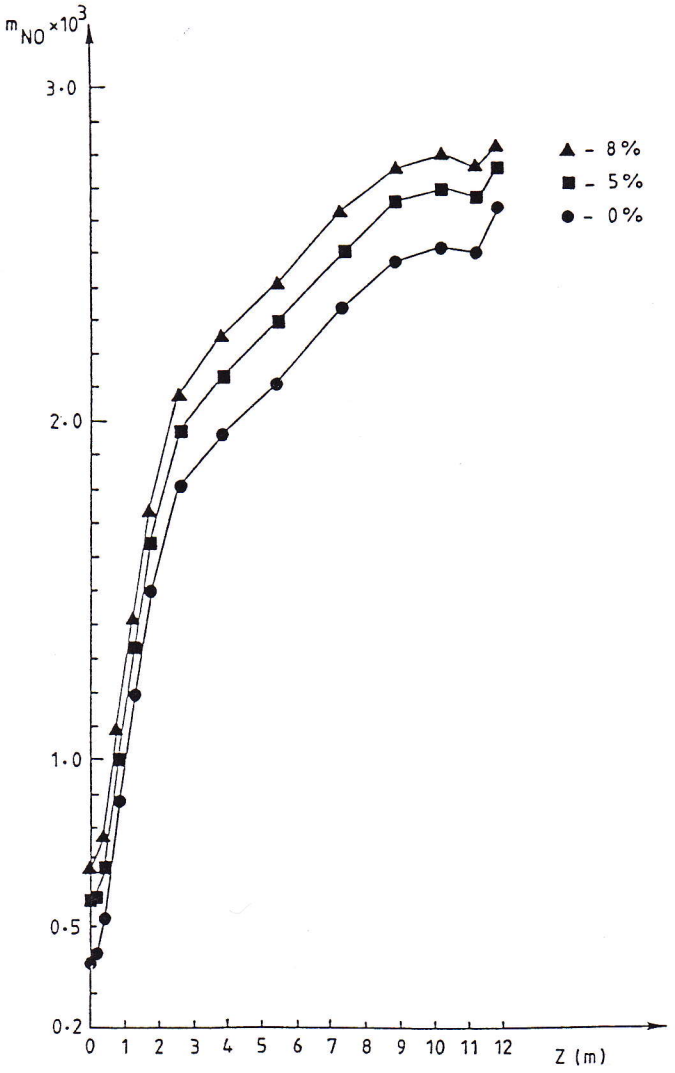

Fig.11 Average value for the X and Y plane for the NO mass concentration along Z direction (kg_{NO}/kg_{mix}) for three excess air levels (0%, 5% and 8%).

Fig.11 shows the average NO mass concentration distribution inside the furnace along the Z direction, for three different excess air levels (0%, 5% and 8%). From Fig.11 it is evident that NO production rate increases along with the excess air for the present simulation, because of the increase of temperature that is the dominant factor in the production of NO.

5.6 Concluding remarks

The present paper describes a prediction procedure for the calculation of the flow, heat-transfer and combustion processes inside a three-dimensional industrial furnace. The incorporation of the modelling for the reverse reactions of the Zeldovich mechanism for the emission of NO forms its novel content.

The results of previous studies suggest that the combustion/aerodynamics and the heat transfer are probably fairly well predicted. The NO modelling relies on equilibrating the oxygen-atom concentration. This has proved justifiable in gas-turbine applications, where the pressures are very high; we assume that it is also realistic for glass furnaces, where the temperatures are high. The predicted NO emissions levels are consistent with recognised industry values, although detailed comparisons are not at present possible because of the lack of reliable real data or to the proprietary nature of those in existence. The dominant region for NO formation in glass furnaces is the edge of the flame. The

6 References

1 GLASSMAN I. Combustion, UK edition. Academic Press Inc (London) Ltd, 1977.

2 ZELDOVICH Y B, SADOVNIKOV P Y and FRAND-KAMENETSKII D A. Oxidation of nitrogen in combustion (trans M Shelef). Academy of Sciences of USSR. Institute of Chemical Physics, Moscow-Leningrad, 1947.

3 WESTENBERG A A. Kinetics of NO and CO in lean, premixed hydrocarbon air flames. *Comb Sci and Tech*, 1971, **4**, p 59.

4 BOWMAN C T. Kinetics of nitric oxide formation in combustion processes. 14th symp (int) on Combustion, The Combustion Institute, 1973, p 729.

5 FLOWER W L, HANSON, R K and KRUGER C H. Kinetics of the reaction of nitric oxide with hydrogen. 15th symp (int) on Combustion. The Combustion Institute, 1975, p 823.

6 DRAKE M C, PITZ R W, CORREA S M and LAPP M. Nitric oxide formation from thermal and fuel-bound nitrogen sources in a turbulent nonpremixed syngas flame. 20th symp (int) on Combustion. The Combustion Institute. 1984a, p 1983.

7 DRAKE M C, PITZ R W, LAPP M, FENIMORE C P, LUCHT R P, SWEENEY, D W and LAURENDEAU N M. Measurements of super-equilibrium hydroxyl concentrations in turbulent non premixed flames using saturated fluorescence. 20th symp (int) on Combustion. The Combustion Institute, 1984b, p 327.

8 DRAKE M C, CORREA, S M, PITZ R W, SHYY W and FENIMORE C P. Super-equilibrium and thermal nitric oxide formation in turbulent diffusion flames. *Comb Flame*, 1987, **69**, p 347.

9 FENIMORE C P. Formation of nitric oxide in premixed hydrocarbon flames. 13th symp (int) on Combustion. The Combustion Institute, 1971, p 373.

10 KATSUKI M and MIZUTANI Y. A simplified reactive flow model of gas tur-

11 PETERS N. An asymptotic analysis of nitric oxide formation in turbulent diffusion flames, *Comb Sci and Tech*, 1978, **17**, p 39.
12 JONES W P and PRIDDIN C H. Predictions of the flowfield and local gas composition in gas turbine combustors. 17th symp (int) on Combustion. The Combustion Institute, 1978, p 399.
13 AHMAD T, PLEE S L and MYERS J P. Computation of nitric oxide and soot emissions from turbulent diffusion flames. Trans ASME, *J Eng Gas Turbines Power*, 1985, **107**, p 48.
14 LAUNDER B E and SPALDING D B. Mathematical models of turbulence. Academic Press, New York, 1972.
15 GOSMAN A D, LOCKWOOD F C, MEGAHED I E A and SHAH N G. The prediction of the flow, reaction and heat transfer in the combustion chamber of a glass furnace. AIAA 18th Aerospace Sciences Meeting, California, 1980.
16 WILLIAMS F A and LIBBY P A. Some implications of recent theoretical studies in turbulent combustion. AIAA, 1980, Paper No. 80-0012.
17 LOCKWOOD F C and NAGUIB A S. The prediction of the fluctuations in the properties of free, round jet, turbulent diffusion flames. *Comb Flame*, 1975, **24**, p 109.
18 LOCKWOOD F C and SHAH N G. A new radiation solution method for incorporation in general combustion prediction procedures. 18th symp (int) on Combustion. The Combustion Institute, 1981, p 1405.
19 TRUELOVE J S. A mixed grey gas model for flame radiation. AERE Harwell Report No. HL 76/3448/KE, 1976.
20 BAULCH D L, DRYSDALE D D, HORNE D G and LLOYD A C. Evaluated kinetic data for high temperature reactions, Vol. 1, 2 and 3. Butterworth, London, 1973.
21 CARVALHO M G, OLIVEIRA P and SEMIAO V. A three-dimensional modelling of an industrial glass furnace. *J Inst Energy*, 1988, **448**, pp 143-156.

(Paper received January 1989)